Cupric Oxide (CuO) Doped Tin Oxide (SnO_2) MOS Multilayer CO_2 Gas Sensor

***Mankar S.S., **Lamdhade G.T., **Raulkar K.B**

**Department of Physics, Shivramji Moghe Arts, Commerce and Science College, Kelapur, Pandharkawada, Dist. Yavatmal, M.S. India*

***Department of Physics, Vidya Bharati Mahavidyalaya, CK Naidu Road, Amravati, M.S. 444 602 India*

DOI:10.37648/ijrst.v13i03.013

[1]*Received: 14 August 2023; Accepted: 18 September 2023; Published: 23 September 2023*

ABSTRACT

Nanoparticles of cupric oxide and tin oxide are synthesized via liquid-phase method. The samples are prepared in the form of multilayer thick films by screen printing technique having based of alumina, samples having different mol % of tin oxide and copper oxide.

CO_2 gas concentration increases from 600 ppm to 1500 ppm, there is little increase of sensitivity, from 600 ppm to 1100 ppm, sensitivity increases linearly and becomes maximum at 1100 ppm. With further increase in CO_2 gas concentration, sensitivity increases by little amount. The XRD pattern of (CuO-SnO_2) system samples show nanocrystalline form and found the desired peaks of composites. FESEM study reveals that the grain size of nanometer order and shows nano- porous structure, which leads to exhibit large surface area, stability and highest response to CO_2 gas. The response time is faster than recovery time. The sample A3 sensor (15CuO:85SnO_2) offers high sensitivity, rapid response and recovery to CO_2 gas.

Keywords: *Nanoparticles; CuO-SnO_2; multilayer thick films; CO_2 Gas Sensors*

INTRODUCTION

Semiconductor gas sensor is known as metal oxide semiconductor gas sensors. Metal oxide Semiconductor sensors (MOS) are also known as chemiresistive gas sensors and have been considered as solid-state gas-sensing materials [1-3]. Khanidtha Jantasom et al. 2013 [4] studied gas sensing properties of SnO_2-CuO Nanocomposites for CO_2 gas. XRD and SEM shows that SnO_2-CuO nanocomposites have a tetragonal and monoclinic structure respectively. It was observed that the nanocomposite products were highly sensitivity to CO_2 gas at room temperature. Satyendra Singh et al. 2014 [5] prepared CuO–SnO_2 nanocomposite by sol–gel route as a sensor by using screen printing methods are used to fabricate thin and thick film samples respectively. For CuO–SnO_2 thick and thin films maximum response. Shravanti Joshi et al. 2015 [6] used simple hydrothermal route method to form heterojunction nanocomposites between p-type CuO and n-type SnO_2 , which nanocomposite exhibited superior sensitivity with short response/recovery times. Fumin Ren et al. 2015 [7] for selectively sensing BTEX (benzene, toluene, ethylbenzene, and xylol) CuO/SnO_2 composites were prepared by a facile microwave-assisted approach. Gas sensing results shows that the sensor based on 3 mol% CuO/SnO_2 composite has the best selectivity and sensitivity. Arindam Das and

[1] How to cite the article: Mankar S.S., Lamdhade G.T., Raulkar K.B. (September 2023); Cupric Oxide (CuO) Doped Tin Oxide (SnO_2) MOS Multilayer CO_2 Gas Sensor; *International Journal of Research in Science and Technology*, Vol 13, Issue 3, 123-133, DOI: http://doi.org/10.37648/ijrst.v13i03.013

Dipankar Panda 2019 [8] prepared functional metal oxide of SnO_2 tailored by CuO via a coprecipitation chemical route followed by annealing in air.

Many metal oxides are suitable for detecting combustible, reducing, or oxidizing gases by conductive measurements Composite metal oxides usually show better gas response than the single component if the catalytic actions of the components complement each other [9-10]. The main purpose of this work was to develop CuO doped SnO_2, nano-crystalline composites sensors which operate at relatively low temperature and sensitive in low possible detection limit with better selectivity.

EXPERIMENTAL

In the present work of paper, we have used sol-gel method (which is under liquid phase synthesis) for the synthesis of pristine nano-particles of CuO, SnO_2 and Al_2O_3 [11-13]. All the chemicals used in this study were of GR grade purchase from Sd-fine, India (purity 99.99%). The chemicals are used without any further purification.

Synthesis of Cupric Oxide (CuO)

In a cleaned round bottom flask, the aqueous solution of $CuCl{:}6H_2O$ (0.2 M) was prepared. After addition of 1 ml of glacial acetic acid to above aqueous solution it was heated to 100ºC with constant stirring. 8 M NaOH was added to above heated solution till its pH attains a value of 7. After this process immediately the color of the solution turned from blue to black and the large amount of black precipitate was obtained. The obtained precipitate was centrifuged and washed 3-4 times with de ionized water. The obtained powder was kept in vacuum oven at 70^0C for 24 hours so as to gets completely dried powder of CuO.

Synthesis of Tin Oxide (SnO_2)

For Synthesis of SnO_2 Stannous chloride dehydrate ($SnCl_2.2H_2O$), Ammonia Solution and de ionised water were used during reaction. All the chemicals used in this study were of GR grades are used without any further purification. 2 g (0.1 M) of stannous chloride dehydrate ($SnCl_2.2H_2O$) was dissolved in 100 ml water. When the complete dissolution occurs about 4 ml ammonia solution was added to this aqueous solution with continuous magnetic stirring. After the 20 minutes of stirring white gel precipitate was formed. This precipitate was allowed to settle for 12 hours. After this it was filtered and by using de-ionised water washed 2-3 times. The obtain precipitate were mixed with 0.27 g activated charcoal (carbon black powder). Then the powder was kept in vacuum oven at 70ºC for 24 hours so as to gets completely dried SnO_2 powder.

Synthesis of Alumina (Al_2O_3)

All chemicals used were analytical grade. Aluminium chloride, $AlCl_3$ (MOLYCHEM), 25% NH_3 solution (QUALIGEN Fine Chemicals) and polyvinyl alcohol (PVA) were used as raw materials for the synthesis of aluminium oxide nanoparticles. 1M alcoholic $AlCl_3$ solution was prepared, followed by addition of 25% ammonia solution. The resulting solution turned to a white sol. This was followed by the addition of PVA (0.5M). The solution was stirred continuously using a magnetic stirrer until it became a transparent sticky gel. The gel was allowed to mature for 24 hours at room temperature. The resultant gel was heat treated at 100°C for 24 hours which led to the formation of light weight porous materials due to the enormous gas evolution. The dried gel was, then calcined at 1000°C for 4 hours and finally, the calcined powders were crushed using mortar and pestle to get the fine homogeneous dense powder of Alumina (Al_2O_3).

Fabrication of Sensors

Three series of the samples prepared were $CuO{:}SnO_2$ with Al_2O_3 base of multilayer sensors. The different combinations are shown in tables 1.

Table 1 Samples Codes of Series: CuO: SnO_2/Al_2O_3/GP

Sr. No.	Sample Codes	Composition of CuO (mole %)	Composition of SnO_2 (mole %)
1	A1	5	95
2	A2	10	90
3	A3	15	85
4	A4	20	80
5	A5	25	75
6	A6	30	70
7	PC	100	0
8	PS	0	100

Out of various methods of sensors preparation, the screen-printing (thick film technology) is most widely used. Screen-printing is the transfer of pastes though a fabric screen onto a substrate.

Multilayer preparation

Fig. 1 (a), and 1(b) show fabrication of interdigited electrodes, actual photographs of interdigited electrodes respectively.

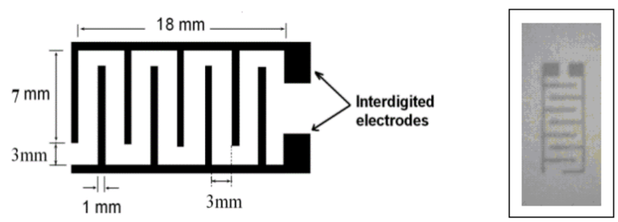

(a) **(b)**

Fig. 1 (a) Fabrication of interdigited Electrodes (b) Actual photograph of interdigited electrodes

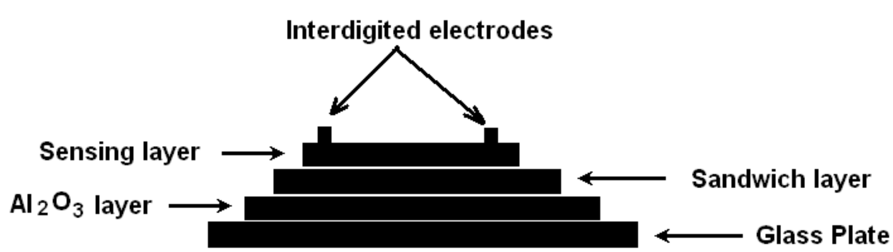

Fig.2 Design of multilayer Sensor

On clean glass plate, Al_2O_3 was deposited by using screen-printing technique and it was used as base of the sensor. On Al_2O_3, the sample layers were prepared. Finally on the top, Interdigited electrodes were fabricated using conducting silver paste as shown in the Fig. 1(b). Design of multilayer sensor is shown in Fig. 2.

Preparation of Samples of Series: CuO: SnO_2 / Al_2O_3/GP

The obtained product of fine nanopowder of CuO and SnO_2 are used for fabrication of thick films sensors by using screen-printing technique. For this, the different X mole% CuO powder (X = 05, 10, 15, 20, 25, 30) was mixed thoroughly with different X mole% of SnO_2 (X = 95, 90, 85, 80, 75, 70) along with Al_2O_3 base on glass plate (GP) substrate the aid of acetone by using the mortar and pestle. The sample codes, mole% of powder, and thickness are listed in the Table 2**..** The mixed powder of CuO : SnO_2 system was further calcinated at temperature 800°C for 5hrs. in the auto-controlled muffle furnace (*Gayatri Scientific, Mumbai, India*.) After, the calcinations again uniformly mixed the powder using the grinder.

Table 2 Thickness of Multi-layers for Series: CuO: SnO_2 / Al_2O_3/GP Gas Sensors.

Sample Code	Composition	Thickness (x 10^{-4} cm)		
	Layers:---- Upper /Al_2O_3/Glass plate (GP)	Upper Layer(1)	Al_2O_3 Layer(2)	Total (1+2)
A1	05CuO:95SnO_2/ Al_2O_3/GP	4.1	29.3	33.4
A2	10CuO:90SnO_2/ Al_2O_3/GP	3.8	28.5	32.3
A3	15CuO:85SnO_2/ Al_2O_3/GP	2.6	29.7	32.3
A4	20CuO:80SnO_2/ Al_2O_3/GP	3.9	28.8	32.7
A5	25CuO:75SnO_2/ Al_2O_3/GP	4.9	28.1	33
A6	30CuO:70SnO_2/ Al_2O_3/GP	4.1	30.2	34.3

Electrical Measurements

Electrical measurements were performed with a Keithley 6487 voltages source cum picoammeter using setup shown in fig. 3. A constant voltage source in the range 1 to 10V is supplied to the sensor electrodes and the current through the sensor measured. The sensor resistance can be calculated by using Ohm's law. The range of voltage used is between $\pm$10 V, in increment of 1V.

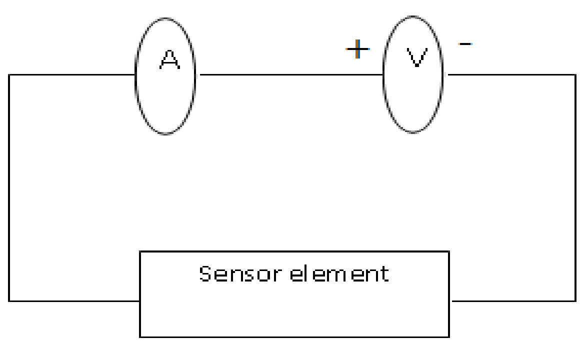

Fig.3 Circuit Configuration of Electrical Measurement

RESULTS AND DISCUSSION

XRD of CuO &SnO_2 Nanomaterial and their dopings

The average crystallite size was calculated by Debye-Scherer's equation with the help of XRD patterns as shown in figure 4. The strong and sharp peak of CuO observed at 37° position with (1 1 1) indicates that the sample is having high crystalline quality, and it is in the structure of monoclinic with lattice parameters a = 0.4685 nm, b = 0.3532 nm, and c = 0.5121 nm, which is good agreement with JCPDS card number 88-2341. The average crystalline size was obtained 27 nm from Debye-Scherer's equation, $D = \frac{K\lambda}{\beta \cos\theta}$

Where, D = nanoparticles crystalline size, K = Scherrer constant (0.98), λ = wavelength and β denotes the full width at half maximum (FWHM).

All the peaks are showing very sharp; it observed that there is no impurities means the prepared sample is having high purity. The peaks position and (h k l) values mentioned, some of the (h k l) values shows bar on the top, it means that the negative direction of the corresponding (h k l). From table 3, it is exhibited that the A3 sample 15CuO:85SnO_2 has small crystalline size [14].

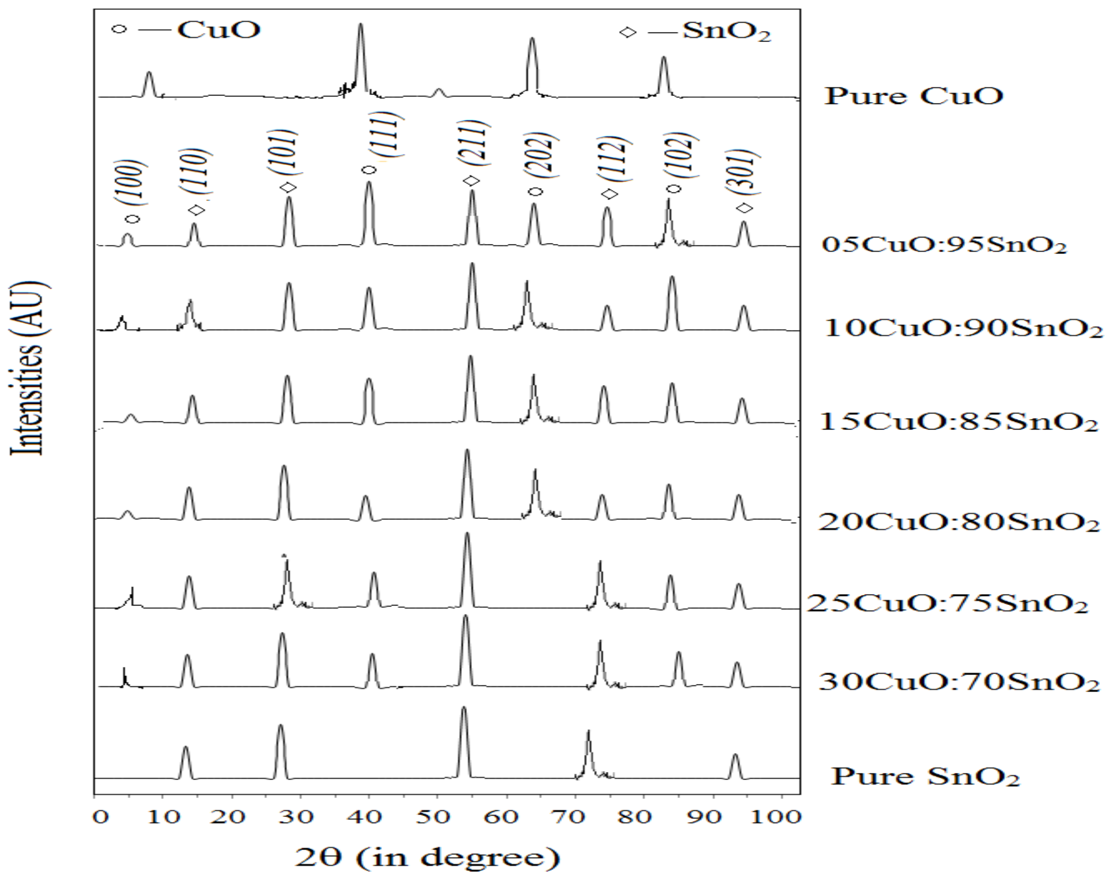

Fig.4. XRD spectra of Pure CuO, Pure SnO_2 and CuO doped with SnO_2 Nanomaterial

Table 3. Average crystallite size of CuO, SnO_2 and doping

Sample Code	Chemical Composition of CuO:SnO_2 (mole %)	Maximum Intensity Peak Position (2θ) degree	FWHM (2θ) degree	Average Crystallite Size (D) in nm
PC	Pure CuO	43.32	0.1865	162.22
A1	05CuO:95SnO_2	49.11	0.2522	122.45

A2	$10CuO:90SnO_2$	54.65	0.1934	153.31
A3	**$15CuO:85SnO_2$**	**55.71**	**0.2312**	**89.65**
A4	$20CuO:80SnO_2$	55.02	0.1832	113.43
A5	$25CuO:75SnO_2$	54.12	0.2433	154.18
A6	$30CuO:70SnO_2$	54.44	0.2132	167.87
PS	Pure SnO_2	53.04	0.2823	132.34

Scanning electron microscopy (SEM) Analysis

From SEM picture (figure 5 (a) to (c)), it is observed that all the samples viz. Al_2O_3, CuO, SnO_2 are porous in nature. Porosity varies with sample to sample and among these material, SnO_2 showed more porosity (small size ~ 60 to 80 nm). Due to small pores size, its surface area is more [11-14] and it shows more sensing nature. Some portion of SEM picture shows some rods with fine voids over them which helps to increase sensing properties. The surface morphology of pure Al_2O_3 , CuO, and SnO_2 , nano materials were studied by SEM and its picture is shown in the Fig. 5

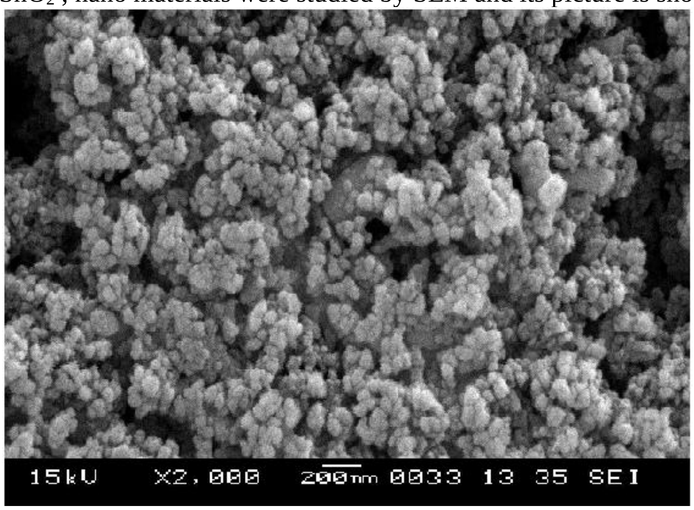

Fig. 5 (a) *SEM picture of Al_2O_3*

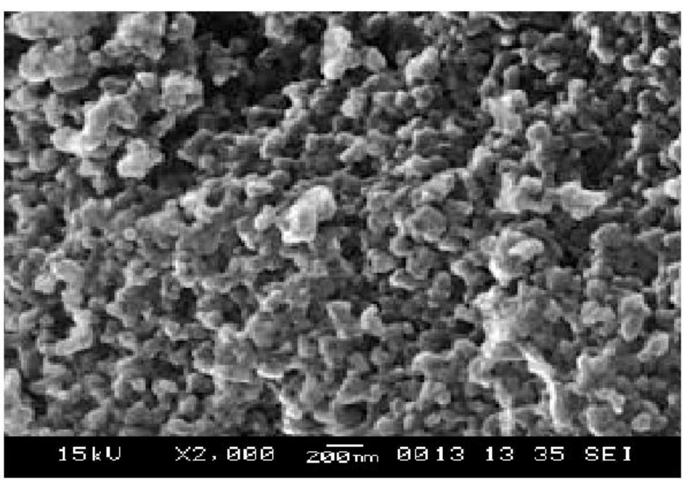

Fig. 5 (b) *SEM picture of CuO*

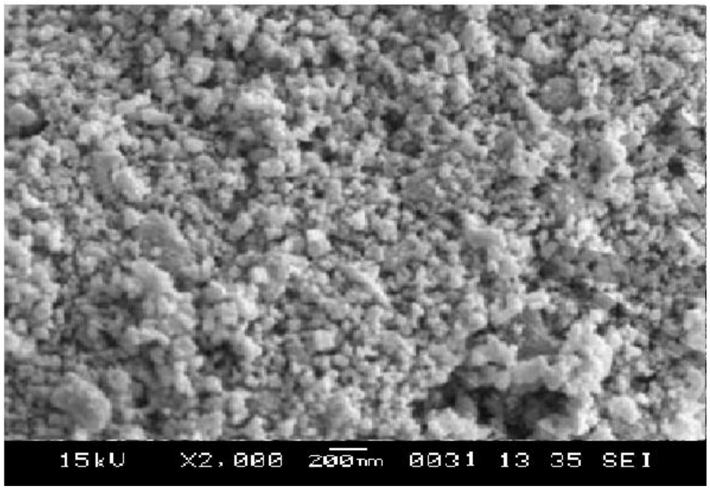

Fig. 5 (c) *SEM picture of* SnO_2

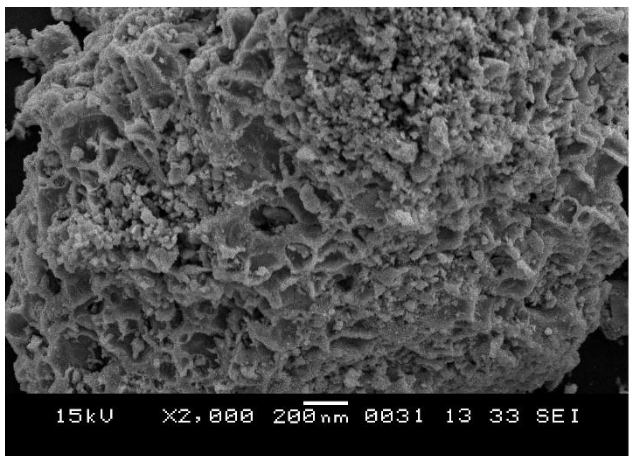

Fig. 6 (a) *SEM picture of* $05CuO:95SnO_2$

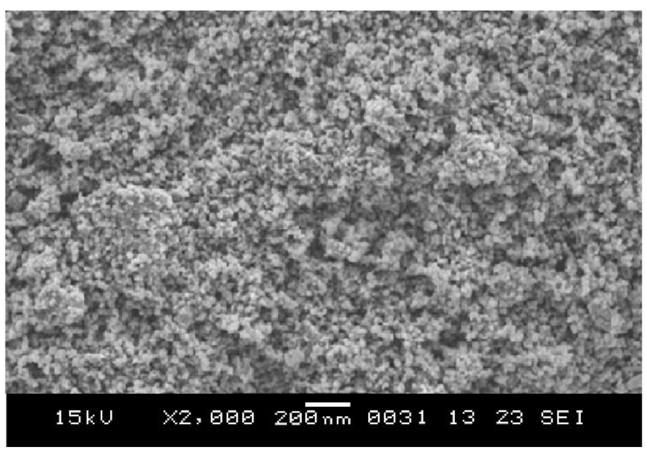

Fig. 6 (b) *SEM picture of* $10CuO:90SnO_2$

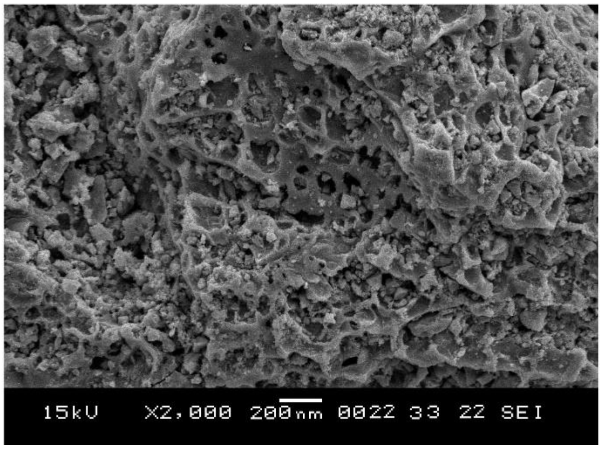

Fig. 6 (c) *SEM picture of 15CuO:85SnO$_2$*

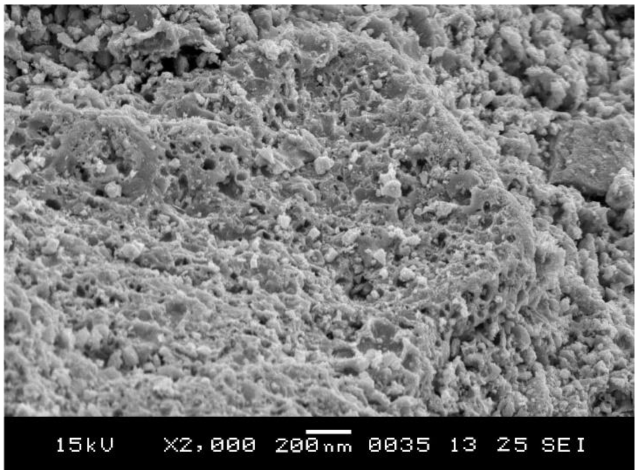

Fig. 6 (d) *SEM picture of 20CuO:80SnO$_2$*

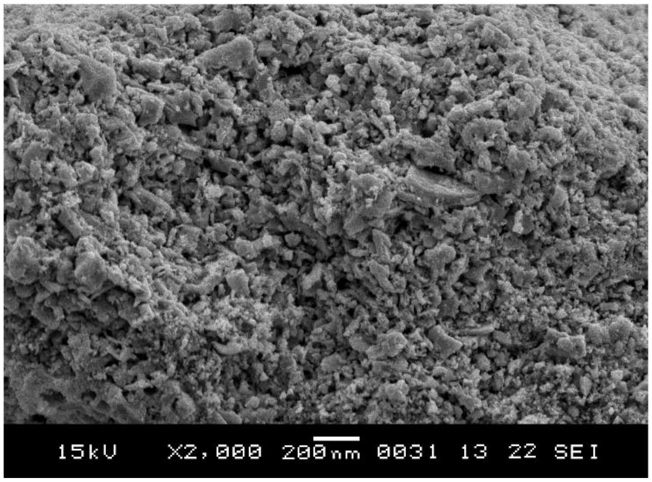

Fig. 6 (e) *SEM picture of 25CuO:75SnO$_2$*

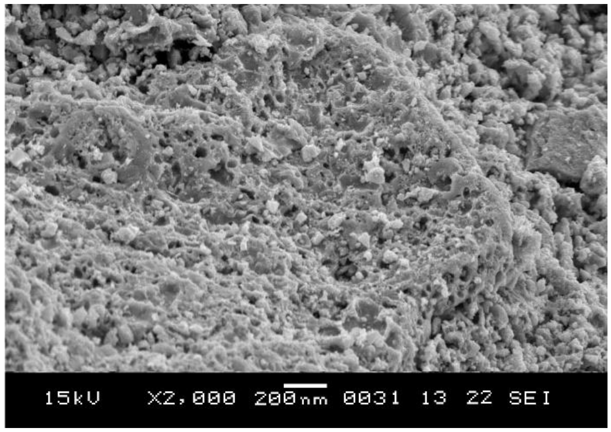

Fig. 6 (f) *SEM picture of 30CuO:70SnO$_2$*

The surface morphologies of pure Al_2O_3, CuO, SnO_2, and their dopings materials were studied by SEM and its picture are shown in the figures 5 to 6. As shown in the SEM pictures, some pores are in the form of rods, some are the form of circles and some are in conical shapes [14].

Table 4. shows the average diameter and number of pores per inch of pure Al_2O_3, CuO, SnO_2, and their dopings.

Table 4. **Average diameter of pore and number of pores per inch of pure samples and their dopings.**

Sample Code	Pure sample and their dopings (mole %)	Average diameter of pore (nm)	Number of pores per inch (in x 2000 magnification)
PA	Al_2O_3	95	154
PC	CuO	80	172
PS	SnO_2	87	160
A1	05CuO:95SnO_2	72	183
A2	10CuO:90SnO_2	78	171
A3	**15CuO:85SnO_2**	**59**	**206**
A4	20CuO:80SnO_2	69	192
A5	25CuO:75SnO_2	65	195
A6	30CuO:70SnO_2	75	157

From the SEM pictures (table 4), it is observed that 15CuO:85SnO_2, have more pores per inch (calculated for x 2,000 magnification for each composition) than other sensors. Thus, these sensors have more active surface areas and exhibit more sensing nature [14-15]. It is also found that average diameter of pore in case of 15CuO:85SnO_2 are small as compared to other doping. This also tends to exhibit large surface area and exhibited high response of the samples.

Detection of CO_2 gas: Gas Sensing Properties

CO_2 acts as an oxidizing agent in some chemical reactions, such as the production of carbonates. It can also participate in redox reactions, where it can accept electrons and become reduced and hence its resistance increases with increase of CO_2 gas concentration [16]. The sensitivity of the sensor is given by,

$$S = \left(\frac{R_{gas} - R_{air}}{R_{air}} \right) = \left(\frac{\Delta R}{R_{air}} \right)$$

Where, R_{gas} = resistance of the sensor in presence of gas and
R_{air} = resistance of the sensor in air

The variations of sensitivities and sensors with concentration of CO_2 gas at room temperature are shown below.

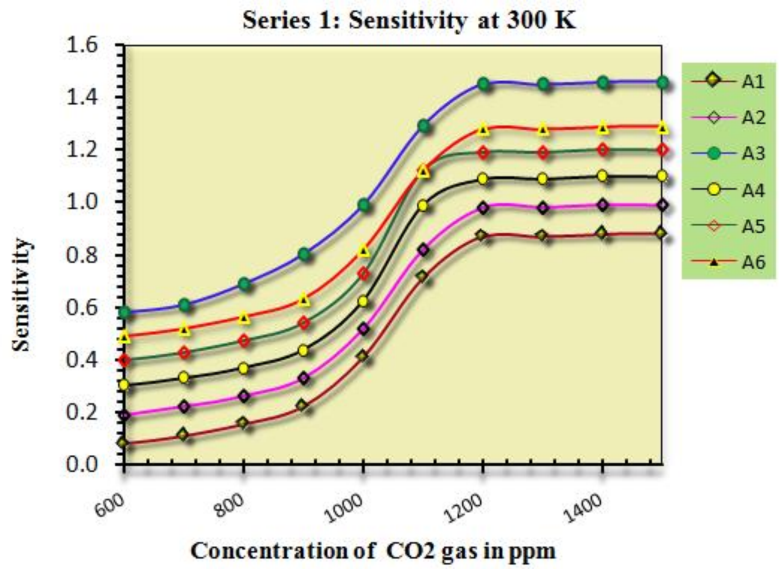

Fig. 7: The variations of sensitivity with CO_2 gas concentration

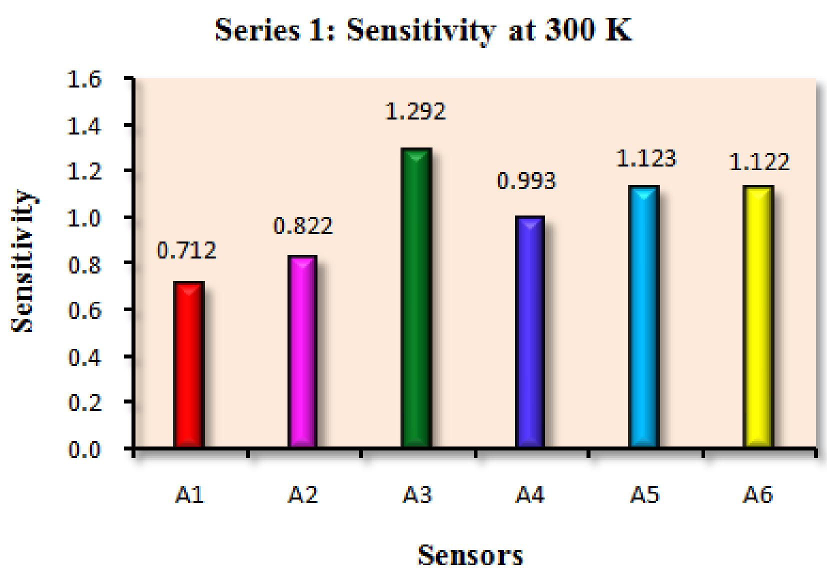

Fig. 8: Sensitivity of different sensors at 1100 ppm

From CO_2 gas detection [17-18] graphs (Fig. 7 and 8) it is observed and manifested that: As CO_2 gas concentration increases from 600 ppm to 1500 ppm, there is little increase of sensitivity, from 600 ppm to 1100 ppm, sensitivity increases linearly and becomes maximum at 1100 ppm. With further increase in CO_2 gas concentration, sensitivity increases by little amount. From Fig. 8, sensitivity was found to be 1.292 (maximum) for A3 sensor (15CuO:85SnO_2) amongst the prepared sensors.

(IJRST) 2023, Vol. No. 13, Issue No. 3, Jul-Sep **e-ISSN: 2249-0604, p-ISSN: 2454-180X**

CONCLUSIONS

The XRD pattern of (CuO-SnO_2) system samples shows nanocrystalline form and found the desired peaks of composites. FESEM study reveals that the grain size of nanometer order and shows nano-porous structure, which leads to exhibit large surface area, stability and highest response to CO_2 gas. The response time is faster than recovery time therefore the A3 sensor (15CuO:85SnO_2) is found to optimized sensor for CO_2 gas.

REFERENCES

1. Chengxiang Wang, Longwei Yin, Luyuan Zhang, Dong Xiang and Rui Gao, 20100, Review Metal Oxide Gas Sensors: Sensitivity and Influencing Factors, Sensors, 10, 2088-2106; doi:10.3390/s100302088
2. G. Korotcenkov, (2014), Handbook of Gas Sensor Materials, doi:10.1007/978-1-4614-7165-3.
3. Nithya Sureshkumar and Atanu Dutta,(2023) Environmental Gas Sensors Based on Nanostructured Thin Films, Multilayer Thin Films - Versatile Applications for Materials Engineering, doi.org/10.5772/intechopen. 89745
4. Khanidtha Jantasom, Suttinart Noothongkaew and Supakorn Pukird, (2013), Synthesis and Gas Sensing Properties of SnO_2-CuO Nanocomposites, Advanced Materials Research Vol. 645, pp 129-132 doi:10.4028/www.scientific.net/AMR.645.129
5. Satyendra Singh, Nidhi Verma, Archana Singh, B.C.Yadav, (2014), Synthesis and characterization of CuO–SnO_2 nanocomposite and its application as liquefied petroleum gas sensor, Materials Science in Semiconductor Processing 18(2014)88–96, http://dx.doi.org/ 10.1016/j.mssp.2013.11.002
6. Shravanti Joshi ,L.Satyanarayana , P.Manjula , Manorama V. Sunkara, (2015), Chemo - Resistive CO_2 Gas Sensor Based on CuO-SnO_2 Heterojunction Nanocomposite Material, Proceedings of the 2015 2nd International Symposium on Physics and Technology of Sensors, Pune,
7. Fumin Ren, Liping Gao, Yongwei Yuan, Yuan Zhang, Ahmed Alqrni, Omar M. Al-Dossary, Jiaqiang Xu, (2015), Enhanced BTEX gas-sensing performance of CuO/SnO_2 Composite, Sensors and Actuators B, http://dx.doi.org/doi:10.1016/j.snb.2015.09.140
8. Arindam Das and Dipankar Panda ,(2019), SnO_2 Tailored by CuO for Improved CH_4 Sensing at Low Temperature, Advanced Science News, Phys. Status Solidi B, 1800296, DOI: 10.1002/pssb.201800296
9. Chengxiang Wang, Longwei Yin , Luyuan Zhang, Dong Xiang and Rui Gao, (2010), Metal Oxide Gas Sensors: Sensitivity and Influencing Factors Sensors, 10, 2088-2106; doi:10.3390/s100302088
10. Ali Mirzaei, Hamid Reza Ansari, Mehrdad Shahbaz, Jin-Young Kim, Hyoun Woo Kim and Sang Sub Kim, (2022), Metal Oxide Semiconductor Nanostructure Gas Sensors with Different Morphologies, Chemosensors, 10, 289. doi.org/10.3390/chemosensors10070289
11. K. B. Raulkar, (2019), Study on sensitivity of nano SnO_2 -ZnO composites with and without PPy layer for sensing CO_2 gas, 2019, Materials Today: Proceedings 15, 604–610.
12. Dmitry Bokov, Abduladheem Turki Jalil, Supat Chupradit, Wanich Suksatan, Mohammad Javed Ansari, 6 Iman H. Shewael, Gabdrakhman H. Valiev, and Ehsan Kianfar, (2021), Review Article, Nanomaterial by Sol-Gel Method: Synthesis and Application, Advances in Materials Science and Engineering Volume 2021, https://doi.org/10.1155/2021/5102014
13. Zahrah Alhalili, (2023), Review Metal Oxides Nanoparticles: General Structural Description, Chemical, Physical, and Biological Synthesis Methods, Role in Pesticides and Heavy Metal Removal through Wastewater Treatment, Molecules, 28, 3086. https://doi.org/10.3390/molecules28073086
14. Tai H., Wang S., Duan Z. and Jiang Y., (2020). Evolution of breath analysis based on humidity and gas sensors: Potential and challenges, Sens. Actuators B Chem., 318, 128104.
15. Nakhleh, M.K., Amal H., Jeries R., Broza Y.Y., Aboud M., Gharra A., Ivgi H., Khatib S., Badarneh S. and Har-Shai, L., (2017). Diagnosis and Classification of 17 Diseases from 1404 Subjects via Pattern Analysis of Exhaled Molecules, ACS Nano, 11, 112–125.
16. Hua B. and Gaoquan S., (2007). Gas Sensors Based on Conducting Polymers, Sensors, 7, 267-307
17. Capone S., Forleo A., Francioso L., Rella R., Siciliano P., Spada- vecchia J., Presicce D.S. and Taurino A.M. (2003), Solid state gas sensors: state of the art and future activities, Journal of Optoelectronics and Advanced Materials 5, 5, 1335 – 1348.
18. Garg R., Kumar V., Kumar D., and Chakarvarti S.K., (2015). Polypyrrole Microwires as Toxic Gas Sensors for Ammonia and Hydrogen Sulphide, Columbia International Publishing Journal of Sensors and Instrumentation, 3, 1-13.